GSC Biological and Pharmaceutical Sciences
eISSN: 2581-3250 CODEN (USA): GBPSC2
Cross Ref DOI: 10.30574/gscbps
Journal homepage: https://gsconlinepress.com/journals/gscbps/

(RESEARCH ARTICLE)

Check for updates

Real-time surveillance of zoonotic and pig pathogens using surface-enhanced Raman scattering system

Yu-Hsing Lin [1, #], Ya-Ling Cyue [2, #], Pi-Hsin Chen [2, #], Shao-Qun Lai [3], Yu-Ying Fang [2] and Shao-Wen Hung [2, 4, *]

[1] *Department of Pet Healthcare, Yuanpei University of Medical Technology, Xiangshan, Hsinchu 300, Taiwan.*
[2] *Division of Animal Industry, Animal Technology Research Center, Agricultural Technology Research Institute, Xiangshan, Hsinchu 300, Taiwan.*
[3] *Division of Animal Resources, Animal Technology Research Center, Agricultural Technology Research Institute, Xiangshan, Hsinchu 300, Taiwan.*
[4] *Department of Nursing, Yuanpei University of Medical Technology, Xiangshan, Hsinchu 300, Taiwan.*
[#] *Contributed equally to this work.*

GSC Biological and Pharmaceutical Sciences, 2024, 26(03), 190–204

Publication history: Received on 16 February 2024; revised on 25 March 2024; accepted on 28 March 2024

Article DOI: https://doi.org/10.30574/gscbps.2024.26.3.0107

Abstract

The shift towards large-scale intensive pig farming methods has led to an increase in cases of complex, mixed infections, and secondary infections. Early diagnosis and disease prevention have become crucial for effective pig farm management. However, clinical diagnosis may be complicated by antibiotic treatment and atypical disease symptoms. To ensure accurate pathology diagnosis, it is essential to integrate robust laboratory diagnostics with traditional methods. Surface-enhanced Raman scattering (SERS) spectroscopy has emerged as a potentially powerful technique for whole-organism fingerprinting, enabling rapid identification of bacteria. Biosensors utilizing SERS offer promising capabilities for sensitive and quick detection of bacterial pathogens, thus reducing diagnosis time. In this study, we aimed to characterize and evaluate a SERS-based diagnostic system for detecting and identifying bacteria in specific pathogen free (SPF) mice, focusing on two bacterial zoonoses and swine bacteria present in pooled swine sera, feces, and meat. We compared the spectra of bacteria recovered from the specimens to those of pure cultured bacteria and conducted principal component analysis to determine the bacterial molecular fingerprint. Our results demonstrated successful detection, identification, and classification of these bacteria in mice specimens (sera and feces) and swine specimens (sera, feces, and meat) using SERS. SERS provided reproducible molecular spectroscopic signatures suitable for analytical applications. This approach presents a new and potent tool for real-time surveillance of animal bacterial pathogens in clinical settings.

Keywords: Animal Diseases; Raman Spectrum; Real-Time Surveillance; Surface Resonance Effect; Zoonotic and Pig Pathogens

1. Introduction

With the intensification and increasing scale of the pig breeding industry, pig disease problems have become increasingly complex, with more cases of mixed infections or secondary infections. Therefore, rapid diagnosis and early prevention of diseases demonstrate their importance. Additionally, the use of antibiotics and vaccines has led to atypical symptoms of bacterial or viral diseases in pigs, often causing significant economic losses for livestock producers. Thus, relying solely on clinical symptoms for rapid diagnosis would be challenging. Strengthening and developing new laboratory diagnostic techniques are currently the primary choice. Therefore, the development of non-invasive real-time spectrum monitoring systems is indeed necessary [1-5].

* Corresponding author: Shao-Wen Hung

Raman spectrometer is an instrument used to measure Raman scattering spectra. Raman scattering light, discovered by Indian scientists in 1928, differs slightly from conventional laser scattering light in that its wavelength varies slightly from the original incident light due to collisions with molecules, causing changes in photon energy due to molecular bonds and structures. Therefore, this technology is widely used in detection in various fields such as high molecular polymers, nano-materials, electrochemistry, semiconductors, thin films, mineralogy, and carbides. In the recent years, due to advancements in charge-coupled device and lasers, scientists have gradually applied Raman spectrometers to rapid biological detection and medical drug testing. Currently, surface-enhanced Raman scattering (SERS), used to enhance the signal required for specific analyses, is increasingly being applied in life science research, including pharmaceuticals, clinical experiments, cell research, immunology, protein group research, genetics, genetic engineering, plastic surgery, biomedical materials, environmental engineering, and biosafety. In the field of life sciences research, Raman spectrometers can identify and differentiate samples with single-cell precision. Instruments combining Raman spectroscopy with microscopic imaging technology will bring great benefits to the life sciences field. Additionally, instruments combining atomic force microscopy with tip-enhanced Raman spectroscopy have emerged in nano-resolution research and analysis [6-10].

With the advancement of technology, there is increasing understanding of SERS. The SERS effect refers to the phenomenon where, on specially prepared metal conductor surfaces or sols, the electromagnetic field near the surface or near the surface is enhanced within the excitation region, leading to enhanced Raman scattering signals of adsorbed molecules compared to normal Raman scattering signals. Furthermore, SERS can obtain structural information that is difficult to obtain with conventional Raman spectroscopy and is widely used in studying surface materials, interfacial surface states, configurations of small biological molecules, molecular conformations, structural analysis, etc., and can analyze compound adsorption orientation at interfaces, changes in adsorption states, and interface information. As for substrates, gold, silver, copper, and a few extremely rare alkali metals (such as lithium and sodium) are known to have strong SERS effects, with gold, silver, and copper requiring surface roughening treatments to exhibit high SERS effects. With the advancement of nano-coating technology, substrate preparation techniques have also improved, resulting in enhanced SERS signals. Therefore, the application of SERS is also receiving increasing attention [11-13].

The characteristic peaks detected by Raman spectrometers are called "characteristic peaks". Since the composition and structure of organisms differ, the characteristic peaks of different species are also different. Even variations in protein or peptide chains caused by genetic changes can be distinguished without molecular biology testing. Changes in the proportion of characteristic peak values can also help track differences in RNA or protein expression. Additionally, Raman spectrum technology can be used to track the location of drugs or determine their efficacy [14].

To break through the limits of biological detection, the combination of biomedicine and optoelectronics has become one of the focus areas of global biotechnology development. Raman spectroscopy, with advancements in optoelectronic technology, can further be used to detect the molecular-level mechanisms, functions, and structures of cells. The SERS technology platform within the surface plasmon effect shows high potential and can be used for developing clinical pathogen rapid identification detection systems in the future. It may even extend to new drug development, cancer medicine, food testing, qualitative and quantitative analysis of microbial metabolites, etc. The development of SERS in the human medical system has successfully been applied in laboratory experiments for the detection of bacteria, viruses, and malaria, with significant effects, achieving detection limits as low as one bacterium, and completing detection in just 5 minutes. From the above literature, SERS has the potential to be applied in clinical pathogen detection and significantly reduce the time required for testing. Currently, traditional methods for detecting animal diseases, including enzyme-linked immunosorbent assay, indirect immunofluorescence antibody method, and traditional polymerase chain reaction, are stable but time-consuming, often taking hours to days. Given the above findings, SERS has the potential to replace traditional detection methods in the future, and there are still no precedents for SERS application in the field of clinical animal health management [16-20]. Therefore, this study attempts to apply SERS for the first time in animal health management, aiming to determine the infection status of animals and the prevalence of diseases in breeding facilities. It also seeks to control the spread of diseases at an early stage and conduct surveillance of animal epidemics.

2. Material and Methods

2.1. Chemicals and Reagents

10% Formalin (Cayman, CAS 50-07-7, Item No.11435), Giemsa Stain Kit (Beso Enterprise, WGO-020), phosphate-buffered saline (PBS; Sigma-Aldrich, Cat. No. P3813), Saline (Shindong Biotech Co., Ltd.), Zoletil 50 (Virbac) were used in this study. Related culture media, API® STAPH, and API® 20 NE were purchased from Creative Life Science Co., Ltd. (New Taipei City, Taiwan).

2.2. Preparation of Pathogens

Staphylococcus aureus (ATCC® 6538), *Pseudomonas aeruginosa* (ATCC® 9027), *Salmonella choleraesuis* (ATCC® 12011), *Salmonella typhimurium* (ATCC® 13311), *Actinobacillus pleuropneumoniae* (ATCC® 55454), and *Bordetella bronchiseptica* (ATCC® 19395) were purchased from ATCC. The cultivation methods for all organisms were conducted following the recommended protocols by American Type Culture Collection (ATCC) (https://www.atcc.org/products/all/6538.aspx#culturemethod, https://www.atcc.org/Products/All/9027-MINI-PACK.aspx#culturemethod, https://www.atcc.org/products/all/12011.aspx#culturemethod, https://www.atcc.org/products/all/13311.aspx#culturemethod, https://www.atcc.org/products/all/55454.aspx#culturemethod, https://www.atcc.org/products/all/19395.aspx#culturemethod).

2.3. Experimental Animals and Animal Welfare

SPF male C57BL/6Narl mice aged 6-8 weeks were studied from the National Laboratory Animal Center, Taipei, Taiwan. The mice were housed in individual ventilated cages with a 12-hour light-dark cycle and controlled temperature (24-27°C) and humidity (50-70%). The animal care and experimental procedures were conducted in accordance with the guidelines set by the Institutional Animal Care and Use Committee (IACUC) of Agricultural Technology Research Institute, with the approval number 106112.

2.4. Establishment of a Known Bacterial-SPF Mouse Platform

2.4.1. Experimental Animals and Grouping

SPF male C57BL/6Narl mice were divided into control group, *Staphylococcus aureus* single-bacterium group, *Pseudomonas aeruginosa* single-bacterium group, and dual-bacterium group infected with *Staphylococcus aureus* or/and *Pseudomonas aeruginosa*. Each group of mice was housed in the individually ventilated caging (IVC) systems.

2.4.2. Administration of Bacterial Pathogens

A single dose of 1×10^6 CFU/0.2 mL of *Staphylococcus aureus* or/and *Pseudomonas aeruginosa* was administered via using oral gavage. The control group was administered an equivalent volume of PBS via using oral gavage.

2.4.3. Clinical Observation

After bacterial challenge, daily clinical observations were conducted, and the severity of symptoms was recorded according to a clinical symptom scoring system. The scoring criteria included body weight (scored from 0 to 3 based on weight loss), body posture (scored from 0 to 3 based on posture abnormalities), piloerection (scored from 0 to 3 based on fur erection), tremors (scored from 0 to 3 based on tremors), social behavior (scored from 0 to 2 based on interaction with other mice), and response to stimuli (scored from 0 to 3 based on reactions to external stimuli).

2.4.4. Collection of Mouse Serum and Fecal Samples

Mice were sacrificed 7 days after bacterial challenge, and serum samples were collected for subsequent SERS analysis of *Staphylococcus aureus* or *Pseudomonas aeruginosa*. Fecal samples were collected by massaging the anus. If fecal samples could not be obtained from the anus, they were collected directly from the rectum or colon by dissection. The collected pathogen or sample specimens were applied to commercially available Raman spectroscopy chips for detection to obtain specific pathogen Raman spectra. Subsequently, a sample database was established or sample testing was conducted according to different settings.

2.4.5. Confirmation of Bacterial Counts

Single bacterial colonies were picked from each fecal sample for confirmation using API® STAPH or API® 20 NE, and the bacterial counts were determined. API® STAPH is a microbial identification kit used for the identification of *Staphylococci* and *Micrococci*, while API® 20 NE is used for the identification of non-fermentative Gram-negative rods/non-*Enterobacteriaceae*. The bacterial suspensions were added to the inoculum using a pipette, and after incubation, the reagents reacted with metabolites to produce color changes, which were then interpreted visually based on the index or analyzed using identification software.

2.5. Polymerase Chain Reaction Detection

The polymerase chain reaction (PCR) assays for *Staphylococcus aureus* and *Pseudomonas aeruginosa* were conducted following the protocols [3, 23], respectively (Table 1). The PCR reaction conditions for *Staphylococcus aureus* and

Pseudomonas aeruginosa were as follows: initial DNA denaturation at 95°C for 5 minutes, followed by 35 cycles of denaturation at 95°C for 45 seconds, annealing at 58°C for 45 seconds, extension at 72°C for 45 seconds, and final extension and completion of DNA strands at 72°C for 5 minutes, with a final temperature return to 4°C. In addition, PCR assays for *Salmonella choleraesuis*, *Salmonella typhimurium*, *Actinobacillus pleuropneumoniae*, and *Bordetella bronchiseptica* referenced the protocols [21, 35, 47], respectively (Table 1). The PCR reaction conditions for *Salmonella choleraesuis*, *Salmonella typhimurium*, and *Bordetella bronchiseptica* were as follows: initial denaturation at 94°C for 10 minutes, followed by 35 cycles of denaturation at 95°C for 45 seconds, annealing at 56°C for 30 seconds, extension at 72°C for 30 seconds, and final extension and completion of DNA strands at 72°C for 10 minutes, with a final temperature return to 4°C. The PCR amplification conditions for *Actinobacillus pleuropneumoniae* were as follows: initial denaturation at 95°C for 10 minutes, followed by 35 cycles of denaturation at 95°C for 45 seconds, annealing at 53°C for 45 seconds, extension at 72°C for 45 seconds, and final extension and completion of DNA strands at 72°C for 10 minutes, with a final temperature return to 4°C. Finally, the resulting PCR products were subjected to electrophoresis on a 1.5% agarose gel (0.5% syneral gel, Diversified Biotech, Inc., Newton Centre, MA, USA, supplemented with 0.5% agarose, Promega Corporation, Madison, WI, USA), stained with ethidium bromide (Amersco Inc., Solon, OH, USA), and then photographed and analyzed for test results.

Table 1 Primer design of polymerase chain reaction and references of *Staphylococcus aureus*、*Pseudomonas aeruginosa*, *Salmonella choleraesuis*, *Salmonella typhimurium*, *Actinobacillus pleuropneumoniae*, and *Bordetella bronchiseptica*

Microorganism	Sequence (5'→3')	Gene	PCR product sizes (bp)	References
Staphylococcus aureus	F: 5'-GCG ATT GAT GGT GAT ACG GTT-3' R: 5'-AGC CAA GCC TTG ACG AAC TAA AGC-3'	*nuc*	279 bp	[3]
Pseudomonas aeruginosa	F:5'-ATG GAT GAG CGC TTC CGT G-3' R:5'-TCA TCC TTC GCC TCC CTG-3'	*ecfX*	528 bp	[23]
Salmonella choleraesuis	F: 5'-ATG CAA CAT TTG GAT ATC GC-3' R: 5'-TCA TCT CAT TAG CGA CCG-3'	*invB*	408	[47]
Salmonella typhimurium	F: 5'-AGT TAA AGT ACT GTC CCT CC-3' R: 5'-CGA AGA AGT CGG TGT TAC-3'	*ompc*	470	[47]
Actinobacillus pleuropneumoniae	F: 5'-TGG CGA TAC CGG AAA CAG AGT C-3' R: 5'-GCG AAA GGC TAT GGT ATG GGT ATG G-3'	*cpx*	715	[21]
Bordetella bronchiseptica	F: 5'-AGG CTC CCA AGA GAG AAA GGC TT-3' R: 5'-TGG CGC CTG CCC TAT C-3'	*fla*	237	[35]

F: forward; R: reverse

2.6. SERS Sample Preparation

2.6.1. Mouse Fecal Sample Pre-Processing

Fecal samples were processed by adding 0.015 g of the sample to 20 μL of sterile normal saline for reconstitution. After incubating at 4°C for 30 minutes, the mixture was centrifuged at 336 ×*g* at 4°C for 15 minutes to remove fecal debris. The supernatant was collected, and bacterial samples were obtained by centrifuging at 2,100 ×*g* at 4°C for 10 minutes. This process was repeated twice with 500 μL of sterile normal saline. Then, 500 μL of sterilized deionized water was added, followed by centrifugation at 2,100 ×*g* at 4°C for 10 minutes, repeated once. Finally, 10 μL of sterilized deionized water was added for reconstitution before SERS detection.

2.6.2. Mouse Serum Sample Pre-Processing

One hundred μL of serum sample was centrifuged at 2,100 ×*g* at 4°C for 10 minutes, and the supernatant was discarded to collect bacterial samples. This was followed by two washes with 500 μL of sterile normal saline and one wash with 500 μL of sterilized deionized water, each followed by centrifugation at 2,100 ×*g* at 4°C for 10 minutes. After discarding the supernatant, 10 μL of sterilized deionized water was added for reconstitution before SERS detection.

2.6.3. SPF Swine Fecal or Meat Sample Pre-Processing

First, 0.1 g of SPF pig feces or meat samples was mixed with a 10% formalin solution to inactivate the pathogen samples (10^6 CFU/mL) of *Salmonella choleraesuis*, *Salmonella typhimurium*, *Actinobacillus pleuropneumoniae*, and *Bordetella bronchiseptica*. Then, 200 μL of sterile normal saline was added for resuspension and homogenization, followed by incubation at 4°C for 30 minutes. After centrifugation at 336 ×*g* at 4°C for 15 minutes, the supernatant was collected to remove fecal impurities. Subsequently, centrifugation was performed at 2,100 ×*g* at 4°C for 10 minutes, and the supernatant was discarded to collect the bacterial sample from the liquid. This step was repeated twice by adding 500 μL of sterile normal saline and centrifuging at 2,100 ×*g* at 4°C for 10 minutes each time. Then, 500 μL of sterile deionized water was added, and centrifugation was performed at 2,100 ×*g* at 4°C for 10 minutes, repeating this step once. Afterward, 20 μL of sterile deionized water was added for resuspension, followed by filtration through filter paper, and finally, the filtrate was collected for SERS detection.

2.6.4. SPF Swine Serum Sample Pre-Processing

First, 500 μL of SPF pig serum sample was mixed with a 10% formalin solution to inactivate the pathogen samples (10^6 CFU/mL) of *Salmonella choleraesuis*, *Salmonella typhimurium*, *Actinobacillus pleuropneumoniae*, and *Bordetella bronchiseptica*. After centrifugation at 2,100 ×*g* at 4°C for 10 minutes, the supernatant was discarded to collect the bacterial sample from the liquid. Then, 500 μL of sterile normal saline was added, and centrifugation was performed at 2,100 ×*g* at 4°C for 10 minutes, repeating this step twice. Subsequently, 500 μL of sterile deionized water was added, and centrifugation was performed at 2,100 ×*g* at 4°C for 10 minutes, repeating this step once. Afterward, 20 μL of sterile deionized water was added for resuspension, followed by SERS detection.

2.7. Raman Spectrometer Detection

The prepared pathogen suspensions (concentration of each pathogen: *Staphylococcus aureus*: 1.32×10^{11} CFU/mL, *Pseudomonas aeruginosa*: 2.71×10^{11} CFU/mL, *Salmonella choleraesuis*: 1×10^9 CFU/mL, *Salmonella typhimurium*: 1×10^9 CFU/mL, *Actinobacillus pleuropneumoniae*: 1×10^9 CFU/mL, and *Bordetella bronchiseptica*: 1×10^9 CFU/mL) were processed and 2 μL were applied onto the detection chip. Subsequently, analysis was conducted using the 3D Laser Raman Microspectroscopy System Nanofinder 30. The machine conditions were set based on the parameters established by [52] with modifications for this study. The laser wavelength was set to 488 nm, laser power was 1 mW ± 15%, integration time was set to 30-40 seconds, objective magnification was 100×, and the numerical aperture (N.A.) was set to 0.9. Raman spectra of each pathogen were obtained, and the resulting spectra were analyzed to establish a standard reference database for pathogen Raman fingerprinting patterns.

2.8. Statistical Analysis

The SERS analysis software used was 3D Laser Raman Microspectroscopy System Nanofinder 30 spectroscopy software. Additionally, principal component analysis (PCA) using SPSS (Statistical package for the social sciences) statistical software (version 28.0) was employed for data point analysis. PCA is commonly used to reduce the dimensionality of a dataset while preserving as much of the variance as possible. In multivariate analysis, it identifies the major components from the variables in the dataset. PCA works by finding the main components from the data variables (i.e., signal wave data) based on the cumulative proportion of contribution. It mathematically transforms the data into a two-dimensional coordinate system, where the first principal component captures the maximum variance of any projection of the data onto the first axis, and the second principal component captures the second largest variance onto the second axis. PC1 and PC2, representing the two main components, are used as the X and Y axes, respectively, to plot relative data points for observation and analysis.

3. Results

3.1. Comparison of PCR and SERS Results

According to our previous comparison of PCR and SERS results of *Staphylococcus aureus* and *Pseudomonas aeruginosa*. After tenfold serial dilution of the four pure strains, amplification products were not detectable by PCR at dilutions of

10^8 for *Staphylococcus aureus* and 10^7 for *Pseudomonas aeruginosa* [17] (Figures 1A, 1C). SERS detection results showed that for pure *Staphylococcus aureus* treated with 10% formalin were unable to detect characteristic peaks (including peaks at 625, 698, 819, 847, 969, 1,118, and 1,202 cm^{-1}) at a dilution of 10^8; for pure *Pseudomonas aeruginosa* treated with 10% formalin were unable to detect characteristic peaks (including peaks at 493, 678, 986, and 1,080 cm^{-1}) at a dilution of 10^7 [17] (Figures 1B, 1D). In this study, after serial 10-fold dilutions of the four pure bacterial strains, they were subjected to SERS detection and compared with PCR results. PCR detection showed that for the four pure bacterial strains, at dilutions of 10^7, amplification products were no longer detectable for *Salmonella choleraesuis* (Figure 2A), with bands appearing below the expected product likely representing primer dimer formation due to primer interaction in the PCR reaction solution. Similarly, for *Salmonella typhimurium* (Figure 2C) and *Bordetella bronchiseptica* (Figure 2G), amplification products were undetectable at dilutions of 10^7 and 10^8, respectively, with primer dimer formation observed below the expected product bands. For *Actinobacillus pleuropneumoniae* (Figure 2D), amplification products were undetectable at a dilution of 10^6, also with primer dimer formation observed. SERS detection was performed on samples of each strain at a concentration of 100 CFU/mL, and characteristic Raman peaks for *Salmonella choleraesuis*, *Salmonella typhimurium*, *Actinobacillus pleuropneumoniae*, and *Bordetella bronchiseptica* were observed (Figures 2B, 2D, 2F, 2H).

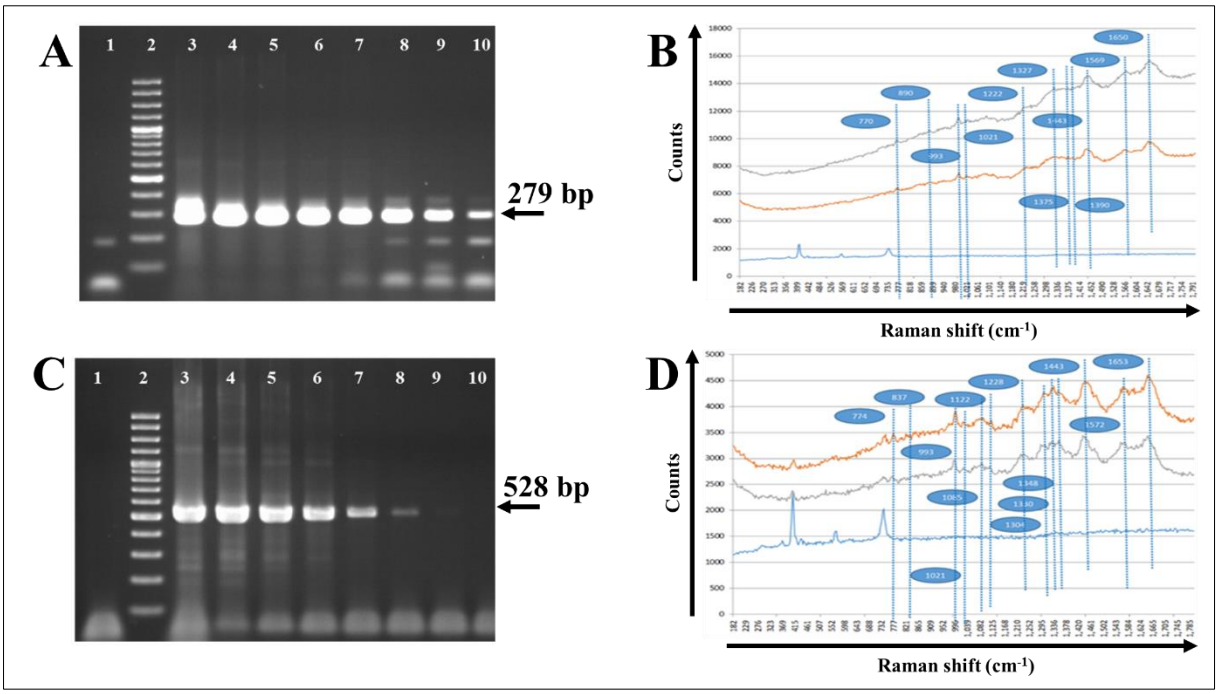

Figure 1 PCR and SERS alignment of SPF mice infected with two zoonotic bacterial pathogen infections. (A) PCR results of *Staphylococcus aureus*; (B) SERS results of *Staphylococcus aureus*; (C) PCR results of *Pseudomonas aeruginosa*; (D) SERS results of *Pseudomonas aeruginosa*. (A & C: Lane 1: negative control; Lane 2: DNA ladder 100 bp; Lane 3: 0× dilution; Lane 4: 10× dilution; Lane 5: 10^2× dilution; Lane 6: 10^3× dilution; Lane 7: 10^4× dilution; Lane 8: 10^5× dilution; Lane 9: 10^6× dilution; Lane 10: 10^7× dilution. B & D: blue line: background; orange and grey lines: sample 1 & 2)

The six pure bacterium strains, *Staphylococcus aureus*, *Pseudomonas aeruginosa*, *Salmonella choleraesuis*, *Salmonella typhimurium*, *Actinobacillus pleuropneumoniae*, and *Bordetella bronchiseptica*, were individually inactivated using a 10% formalin solution as the target pathogens for SERS detection. Subsequently, 2 µL of bacterial suspension was applied onto Raman detection chips for obtaining Raman spectra of the four pathogens. Based on the preliminary test results, wavelengths ranging from 650 to 1,780 were selected for comparing the Raman spectra of each bacterium with those obtained from sterile deionized water (ddH_2O) or 10% formalin solution. The results revealed noticeable differences in Raman shift signal intensity at 11 specific peaks for *Staphylococcus aureus* (1.32×10^{11} CFU/mL), including 770, 890, 993, 1,021, 1,222, 1,327, 1,375, 1,390, 1,443, 1,569, and 1,650 Raman shift (cm^{-1}) (Figure 1B). The noticeable differences in Raman shift signal intensity at 13 specific peaks for *Pseudomonas aeruginosa* (2.71×10^{11} CFU/mL), including 774, 873, 993, 1,021, 1,085, 1,122, 1,228, 1,304, 1,330, 1,348, 1,443, 1,572, 1,653 Raman shift (cm^{-1}) (Figure 1D). Moreover, the noticeable differences in Raman shift signal intensity at 17 specific peaks for *Salmonella choleraesuis* included 640, 716, 777, 843, 896, 996, 1,024, 1,091, 1,119, 1,234, 1,301, 1,327, 1,437, 1,476, 1,566, 1,595, and 1,656 Raman shift (cm^{-1}) (Figure 2A). Similarly, for *Salmonella typhimurium*, 20 distinct peaks exhibited significant differences

in Raman shift signal intensity, including 662, 713, 770, 846, 896, 993, 1,024, 1,076, 1,098, 1,116, 1,165, 1,231, 1,307, 1,327, 1,443, 1,470, 1,564, 1,600, 1,650, and 1,656 Raman shift (cm^{-1}) (Figure 2D). In the case of *Actinobacillus pleuropneumoniae*, 8 noticeable peaks showed differences in Raman shift signal intensity, including 774, 993, 1,231, 1,437, 1,467, 1,566, 1,593, and 1,653 Raman shift (cm^{-1}) (Figure 2F). Lastly, for *Bordetella bronchiseptica*, 7 distinct peaks demonstrated differences in Raman shift signal intensity, including 990, 1,237, 1,324, 1,440, 1,566, 1,604, and 1,648 Raman shift (cm^{-1}) (Figure 2H).

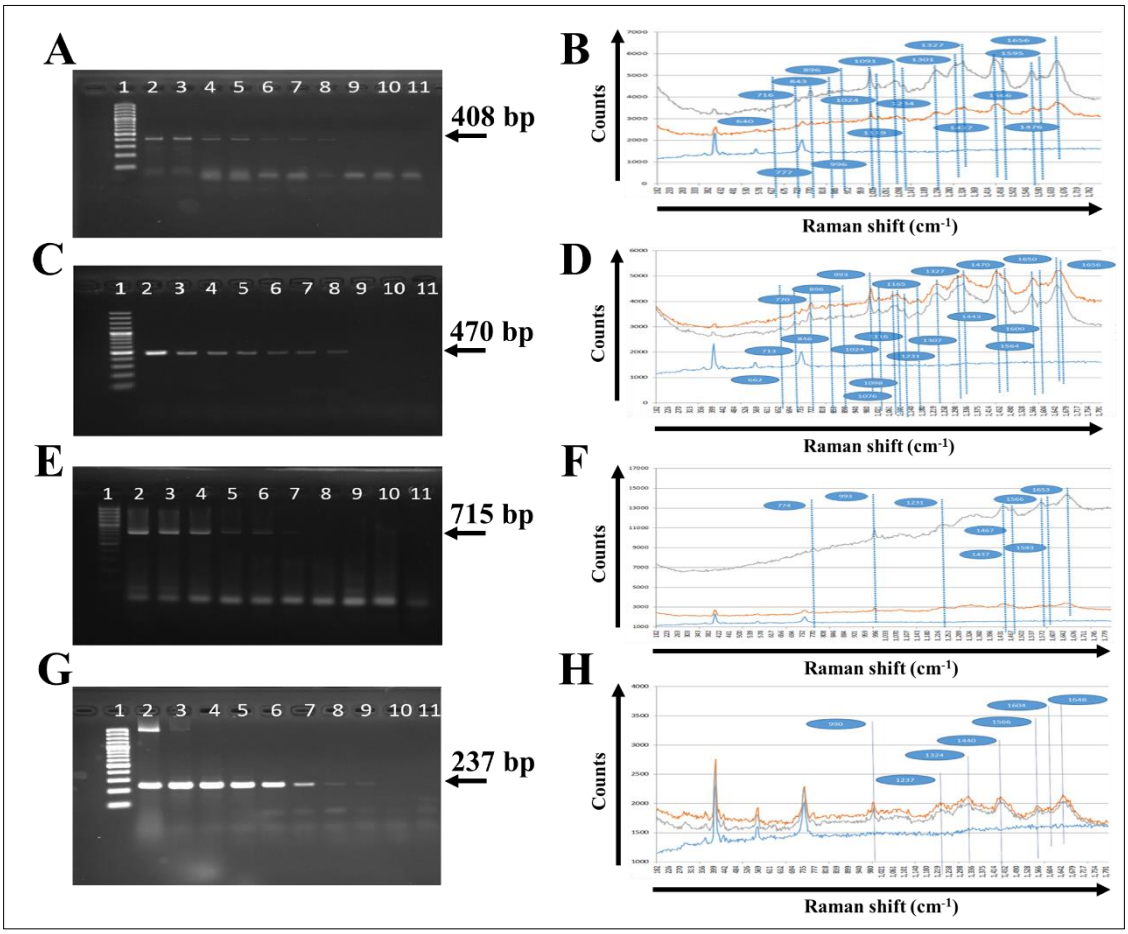

Figure 2 PCR and SERS alignment of four kinds of swine bacteria. (A) PCR results of *Salmonella choleraesuis*; (B) SERS results of *Salmonella choleraesuis*; (C) PCR results of *Salmonella typhimurium*; (D) SERS results of *Salmonella typhimurium*. (E) PCR results of *Actinobacillus pleuropneumoniae*; (F) SERS results of *Actinobacillus pleuropneumoniae*. (G) PCR results of *Bordetella bronchiseptica*; (H) SERS results of *Bordetella bronchiseptica*. (A, C, E, G: Lane 1: DNA ladder 100 bp; Lane 2: 0× dilution; Lane 3: 10× dilution; Lane 4: 10^2× dilution; Lane 5: 10^3× dilution; Lane 6: 10^4× dilution; Lane 7: 10^5× dilution; Lane 8: 10^6× dilution; Lane 9: 10^7× dilution; Lane 10: 10^8× dilution; Lane 11: negative control. B, D, F, H: blue line: background; orange and grey lines: sample 1 & 2)

3.2. Mix of Swine Meat Samples and Pathogens for SERS Detection

Swine meat samples were individually mixed with the fixed bacterium strains (inactivated using 10% formalin) of the following pathogens: *Salmonella choleraesuis*, *Salmonella typhimurium*, *Actinobacillus pleuropneumoniae*, and *Bordetella bronchiseptica*. After mixing, the mixed samples underwent sample pre-processing before being subjected to SERS detection. The results indicated that the characteristic Raman peaks of each bacterium could be detected (Figure 3A). For *Salmonella choleraesuis*, compared to sterile deionized water (ddH_2O) or 10% formalin solution, there were 16 noticeable differences in Raman shift signal intensity, including peaks at 640, 716, 777, 843, 896, 996, 1,024, 1,091, 1,119, 1,234, 1,301, 1,327, 1,437, 1,566, 1,595, and 1,623 cm^{-1} (Figure 3B). Similarly, for *Salmonella typhimurium*, there were 20 noticeable differences in Raman shift signal intensity compared to ddH_2O or 10% formalin solution, including peaks at 662, 713, 770, 846, 896, 993, 1,024, 1,076, 1,098, 1,116, 1,165, 1,231, 1,313, 1,327, 1,443, 1,470, 1,576, 1,600, 1,650, and 1,656 cm^{-1} (Figure 3B). Likewise, for *Actinobacillus pleuropneumoniae*, 8 noticeable differences in Raman shift signal intensity were observed compared to ddH_2O or 10% formalin solution, including peaks at 774, 993, 1,231, 1,437, 1,474, 1,566, 1,593, and 1,653 cm^{-1} (Figure 3B). Lastly, for *Bordetella bronchiseptica*, 7 noticeable differences in

Raman shift signal intensity were observed compared to ddH_2O or 10% formalin solution, including peaks at 990, 1,237, 1,324, 1,440, 1,566, 1,604, and 1,648 cm^{-1} (Figure 3B).

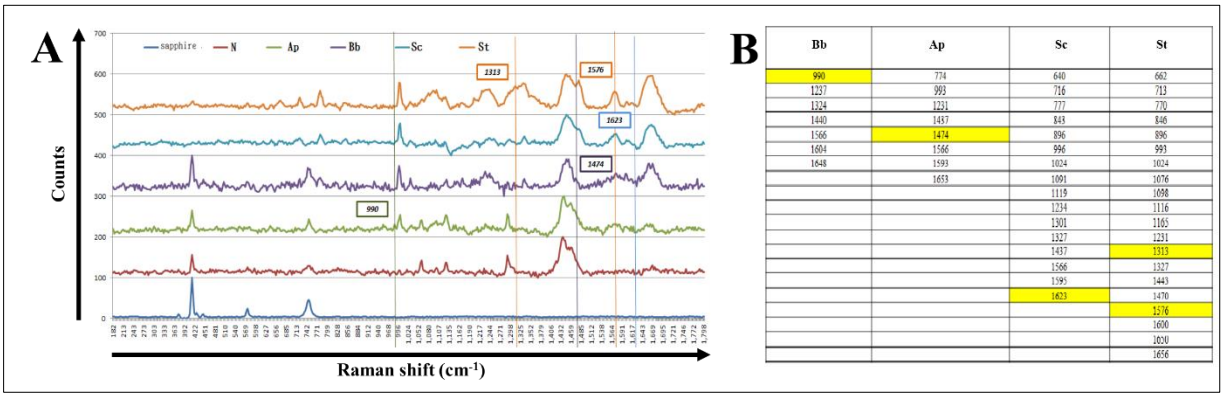

Bb	Ap	Sc	St
990	774	640	602
1237	993	716	713
1324	1231	777	770
1440	1487	843	848
1566	1474	896	896
1604	1566	996	993
1648	1593	1024	1024
	1653	1091	1076
		1119	1098
		1234	1116
		1301	1165
		1327	1231
		1437	1313
		1566	1327
		1595	1443
		1623	1470
			1576
			1600
			1630
			1656

Figure 3 Detection, identification, and classification of four kinds of swine bacteria from swine specimens by using SERS. (A) SERS spectra of bacteria. (B) The characteristic Raman peaks. Sc: *Salmonella choleraesuis*; St: *Salmonella typhimurium*; Ap: *Actinobacillus pleuropneumoniae*; Bb: *Bordetella bronchiseptica*; N: normal pig specimens. Sapphire: background. The highlighted area shows the Raman characteristic peaks compared among the four strains of bacteria

3.3. Establishment of a Known Bacterial Mouse Platform and SERS Detection

After infecting SPF mice, clinical symptom scores recorded over the course of 7 days were all 0, indicating that there were no significant behavioral changes observed in any of the groups of mice due to the infection (data not shown). After completing the pre-processing of fecal samples from known bacteria-infected SPF mice, SERS detection was conducted. The results showed that when mouse feces were artificially inoculated with *Staphylococcus aureus* (1×10^6 CFU/0.2 mL) or/and *Pseudomonas aeruginosa* (1×10^6 CFU/0.2 mL). In the control group, the mice were administrated with an equivalent volume of PBS compared to the other groups. A known bacterial mouse platform was established by feeding specific bacterial strains to mice housed in IVC. In this study, single-target bacteria (*Staphylococcus aureus* or *Pseudomonas aeruginosa*) or dual-target bacteria (*Staphylococcus aureus* and *Pseudomonas aeruginosa*) were orally administered to mice, and feces were collected from each group after 7 days post-challenge. After fecal sampling and streaking, single colonies were selected from each fecal sample and subjected to API® STAPH or API® 20 NE for pathogen confirmation. Clinical symptom scores recorded over the 7-day period following bacterial administration were all zero, indicating no significant behavioral changes in the mice due to bacterial inoculation. Fecal cultures taken 7 days after inoculation showed that in the "single-target bacteria orally administered" group, the fecal bacterial count for *Staphylococcus aureus* was 4.2×10^9 CFU/g, and for *Pseudomonas aeruginosa* was 3.9×10^9 CFU/g. In the "dual-target bacteria orally administered" group, the total bacterial count in the feces was 4.8×10^9 CFU/g, with *Staphylococcus aureus* at 9.3×10^7 CFU/g and *Pseudomonas aeruginosa* at 3×10^7 CFU/g. The total bacterial counts in the control group was 2.2×10^9 CFU/g. In the fecal samples collected before bacterial administration, no characteristic Raman peaks of pathogens were detected (data not shown). However, after 7 days of bacterial administration and sample pre-processing, characteristic Raman peaks were detected in all fecal samples. SERS detection could effectively detect the presence of either *Staphylococcus aureus* or *Pseudomonas aeruginosa* in the feces after sample pre-processing. For the *Staphylococcus aureus* group, 20 characteristic Raman peaks were observed at 783, 827, 859, 929, 1,003, 1,095, 1,114, 1,125, 1,169, 1,292, 1,329, 1,406, 1,450, 1,550, 1,564, 1,576, 1,605, 1,666, 1,717, and 1,761 Raman shift (cm^{-1}); for the *Pseudomonas aeruginosa* group, 23 characteristic Raman peaks were observed at 475, 771, 906, 1,006, 1,036, 1,089, 1,129, 1,169, 1,241, 1,304, 1,337, 1,358, 1,373, 1,379, 1,438, 1,453, 1,462, 1,483, 1,550, 1,579, 1,626, 1,660, and 1,669 Raman shift (cm^{-1}). However, in fecal samples containing dual-target bacteria, some characteristic Raman signals are obscured by other peaks, resulting in the detection of only three characteristic Raman peaks. *Staphylococcus aureus* exhibits two characteristic Raman peaks (detectable at Raman shifts of 929 and 1,329 cm^{-1}), while *Pseudomonas aeruginosa* shows three characteristic Raman peaks (detectable at Raman shifts of 475, 771, and 1,089 cm^{-1}) (Figure 4).

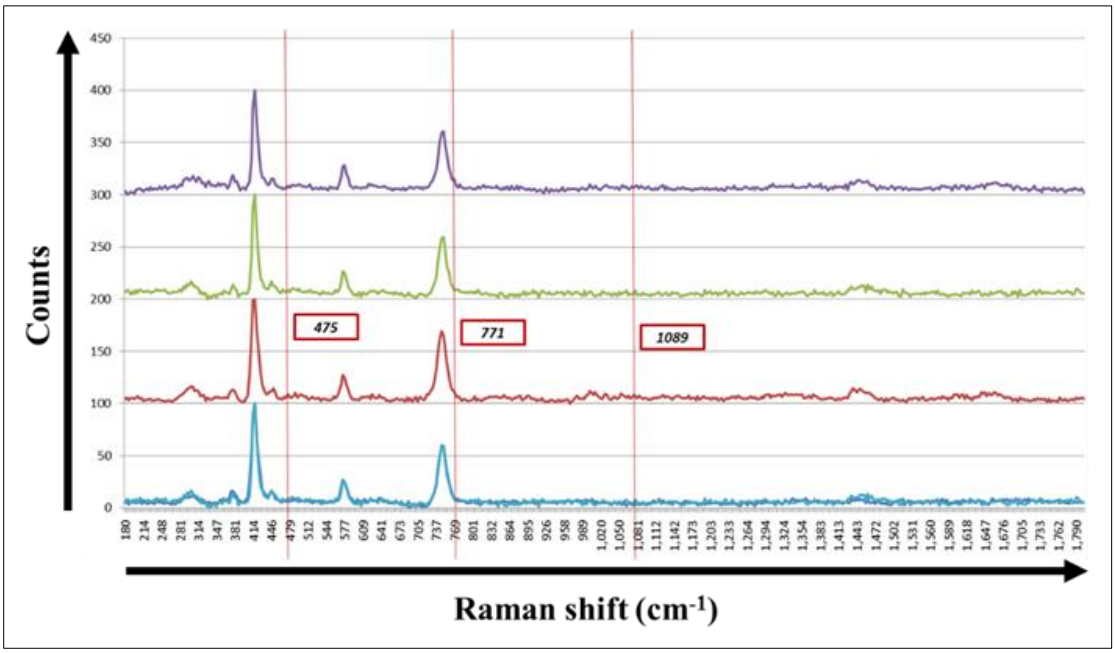

Figure 4 Establishment of a known bacterial mouse platform and SERS detection in mouse fecal samples. After 7 days, Raman characteristic peaks were detected in fecal samples from SPF mice following sample pre-processing. The deep blue line represents the normal group, the light blue line represents the *Staphylococcus aureus* group (Sample I), the red line represents the *Pseudomonas aeruginosa* group, the green line represents the *Staphylococcus aureus* group (Sample II), and the purple line represents the dual-bacterial group of *Staphylococcus aureus* and *Pseudomonas aeruginosa*

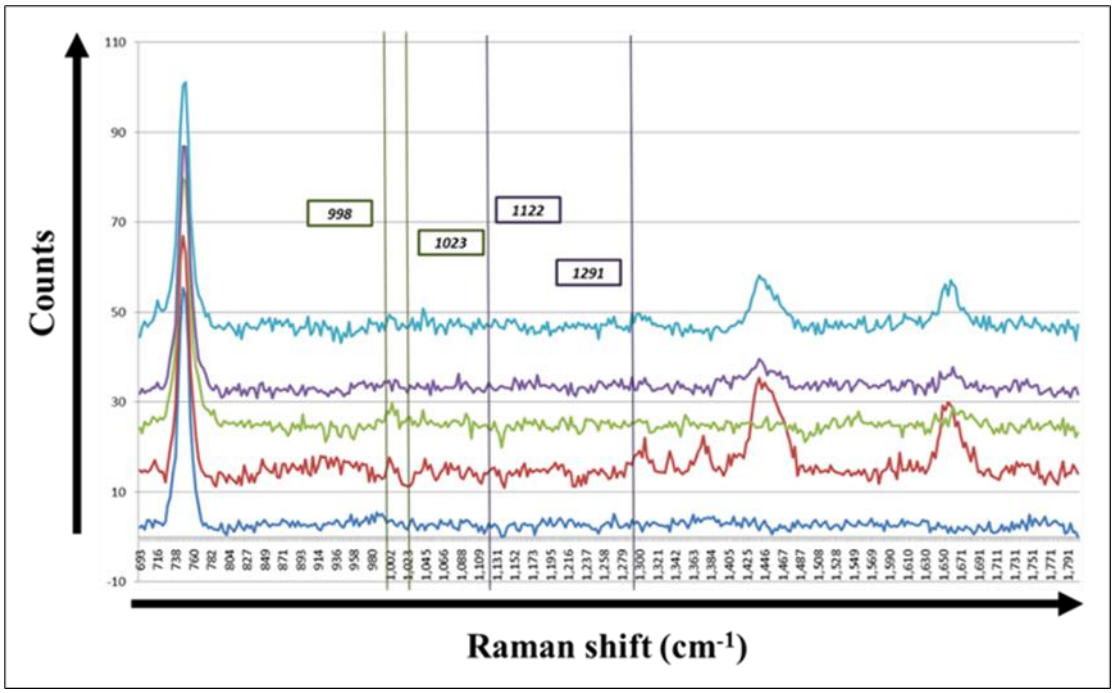

Figure 5 Establishment of a known bacterial mouse platform and SERS detection in mouse serum samples. After 7 days, characteristic Raman peaks were detected in serum samples from SPF mice following sample pre-processing. The deep blue line represents the background values of the SERS detection chip. The light blue line represents the dual-bacterial group of *Staphylococcus aureus* and *Pseudomonas aeruginosa*. The red line represents the normal group. The green line represents the *Pseudomonas aeruginosa* group. The purple line represents the *Staphylococcus aureus* group

After 7 days of bacterial administration and sample pre-processing, characteristic Raman peaks were detected in all serum samples. SERS detection could effectively detect the presence of either *Staphylococcus aureus* or *Pseudomonas aeruginosa* in the sera after sample pre-processing. For the *Staphylococcus aureus* group, 20 characteristic Raman peaks were observed at 783, 827, 859, 929, 1,003, 1,095, 1,114, 1,125, 1,169, 1,292, 1,329, 1,406, 1,450, 1,550, 1,564, 1,576, 1,605, 1,666, 1,717, and 1,761 Raman shift (cm^{-1}); for the *Pseudomonas aeruginosa* group, 23 characteristic Raman peaks were observed at 475, 771, 906, 1,006, 1,036, 1,089, 1,129, 1,169, 1,241, 1,304, 1,337, 1,358, 1,373, 1,379, 1,438, 1,453, 1,462, 1,483, 1,550, 1,579, 1,626, 1,660, and 1,669 Raman shift (cm^{-1}). However, in fecal samples containing dual-target bacteria, some characteristic Raman signals are obscured by other peaks, resulting in the detection of only two characteristic Raman peaks. *Staphylococcus aureus* exhibits two characteristic Raman peaks (detectable at Raman shifts of 1,122 and 1,291 cm^{-1}), while *Pseudomonas aeruginosa* also shows two characteristic Raman peaks (detectable at Raman shifts of 998, and 1,023 cm^{-1}) (Figure 5).

4. Discussion

In recent years, biophotonics has emerged as a key area of focus in global biotechnology, employing optical technologies to detect biological responses, including the mechanisms, functions, and structures at the molecular level of cells [21-25]. In clinical medicine, it offers non-invasive methods for detecting, diagnosing, and treating diseases in humans. Consequently, it represents an interdisciplinary field integrating biomedical sciences, biotechnology, optics, electronics, electrical engineering, information technology, precision mechanics, physics, and chemistry [26-32]. The application of spectroscopy in biophotonics encompasses fundamental biological research, real-time physiological and biochemical monitoring within organisms, and the development of novel methods for disease diagnosis and treatment control [33-35].

Compared to SERS-related research projects in Taiwan, this study represents the first published instance of on-site pathogen detection in pigs using SERS, applying SERS to clinical animal disease detection. Furthermore, due to the relatively complex regulatory restrictions in the veterinary system compared to the human medical system, the industry has shifted its focus towards clinical animal disease detection. Therefore, this study represents an innovative application of SERS from laboratory and human clinical detection to animal disease detection. Ultimately, the findings of this study can be integrated with SERS research results in agriculture, forestry, poultry, aquaculture, and other related fields to establish a Raman spectroscopy database. This database can serve as a platform for rapid detection of diseases in agriculture, forestry, and animal husbandry, facilitating early detection of animal infections and prevailing disease conditions on farms, thereby aiding in disease control and providing necessary certification, quarantine, and epidemic prevention for domestic and international use [36-40].

Currently, SERS is being increasingly used in the human medical system for the detection of bacterial pathogens and the establishment of bacterial strain Raman spectral analyses [17, 41]. These bacterial pathogens include methicillin-resistant *Staphylococcus aureus* and methicillin-sensitive *Staphylococcus aureus* differentiation; *Enterococcus* spp., *Escherichia coli*, *Klebsiella pneumoniae*, *Pseudomonas aeruginosa*, *Proteus mirabilis*. Additionally, SERS has been applied to detect virus strains (such as different strains of influenza viruses), sample detection of hepatitis C virus, and detection of bacteriophages in the laboratory. In parasite detection, SERS has been applied to the detection of Plasmodium in blood samples [42-47]. Currently, SERS has not been applied to clinical animal disease detection. Therefore, the transition of SERS from laboratory and human clinical detection to animal disease detection represents an innovative application. Since the current use of SERS for microbial detection is still in its early stages and lacks established standards, factors such as laser wavelength, laser energy, integration time, and chip material can affect the relative positions of characteristic peak shifts. However, in this study, to achieve a more stable state, we first referred to the work [48-52] and conducted experiments using the same system and conditions. This study attempted to use SERS to detect *Staphylococcus aureus*, *Pseudomonas aeruginosa*, *Mycoplasma hyopneumoniae*, and *Streptococcus suis*. However, since this model is expected to be used on-site to minimize the transmission of pathogens between farms during the pathogen detection process, we attempted to first inactivate the bacteria with 10% formalin. The results showed characteristic Raman peaks of *Staphylococcus aureus* at 625, 698, 819, 847, 969, 1,118, and 1,202; *Pseudomonas aeruginosa* at 493, 678, 986, and 1,080; *Mycoplasma hyopneumoniae* at 554, 669, 731, 815, 1,060, 1,268, and 1,277; and *Streptococcus suis* at 535, 666, 700, 775, 1,006, 1,035, 1,139, and 1,230. Additionally, we attempted to detect *Staphylococcus aureus* and *Pseudomonas aeruginosa* without formalin inactivation and compared the results between the two approaches. It was found that *Staphylococcus aureus* exhibited a decrease in characteristic Raman peaks at 500, 549, 805, 1,039, and 1,280 with formalin inactivation, while *Pseudomonas aeruginosa* exhibited a decrease at 507, 542, and 781. This reduction in characteristic peaks may be due to formaldehyde binding to amino groups in proteins, causing protein coagulation, thereby altering surface composition and resulting in fewer characteristic peaks. However, since most characteristic peaks were retained, in order to reduce the risk of pathogen transmission between farms

during the pathogen detection process, the inactivation of bacterial cells with formalin was still performed in this study [17].

Regarding the comparison between Raman spectroscopy and PCR, the results showed that there was no significant difference in the detection limits of the two methods. However, since Raman spectroscopy has traditionally been used for qualitative analysis, quantitative analysis requires relative quantitative methods for comparison, and there is currently no established method for absolute quantification [48-50]. As pattern matching relies on database matching, this study collected over a hundred Raman data patterns for each bacterial strain to accumulate a database, ensuring that different strains of the same bacteria did not result in differences in characteristic Raman peaks at different time points.

The biophotonics, particularly SERS, has emerged as a promising tool for the detection of pathogens in various fields, including clinical medicine and animal disease detection. While SERS applications have predominantly focused on human medical systems, this study represents a novel application in the field of animal disease detection. By transitioning SERS from laboratory settings to on-site animal disease detection, this study addresses the need for rapid and accurate pathogen detection in agriculture and animal husbandry. Furthermore, by establishing a Raman spectroscopy database integrating data from various fields, this study contributes to the development of a platform for rapid disease detection in agriculture, forestry, and animal husbandry. This platform will be instrumental in early detection and control of diseases in animals, ultimately enhancing animal health and safety measures [51-53].

Additionally, while SERS has shown potential for microbial detection, particularly in distinguishing bacterial strains, its quantitative analysis capabilities require further development. Nevertheless, by accumulating data and establishing a comprehensive database, this study lays the groundwork for future advancements in quantitative analysis using SERS. Overall, the findings of this study contribute to the advancement of biophotonics and its applications in disease detection and control, both in human and animal health sectors.

Due to the potential interference from luminescent substances or other chemical signals during the detection process of Raman spectroscopy, the simulation of Raman spectroscopy technology applied in on-site conditions was conducted on a known bacterial mouse platform. By utilizing a germ-free mouse platform to reduce the variables, attempts were made to test the influence of single and dual bacterial conditions on the signal. The results showed that in the application on biological organisms, the characteristic Raman peaks of bacterial bodies may be masked by interference from sample substances [17]. Furthermore, when further applying Raman spectroscopy technology to the detection of pathogens in a specific pathogen-free (SPF) pig model, the results indicated that fecal samples had a greater interference with Raman spectroscopy technology, while interference from serum and urine samples was relatively lower. Future efforts may focus on reducing interference signals through sample pretreatment [17].

In terms of pattern matching, current methods mostly rely on manual comparison, and when the pattern is smoothed, it becomes difficult to observe, leading to misjudgments. To mitigate the effects of signal interference and human error, the analysis in the laboratory currently emphasizes spot analysis [17]. The basis of spot analysis is principal component analysis, a method for analyzing and simplifying datasets. By combining existing variables to create new variables, the aim is to achieve data reduction while retaining important information from the original data. The results of this study also utilized principal component analysis to plot two-dimensional coordinates using the primary components (PC1 and PC2) for spot analysis, which successfully separated the clustering of six bacterium strains (data not shown). In the future, with more data on other bacterial strains available, cross-plotting can be expanded according to the demand by selecting additional primary components for analysis (e.g., PC1, PC2, PC3, PC4) [17, 54-57].

This study aims to translate the currently used SERS technology in the biomedical field into applications in the livestock industry, thereby developing a rapid, highly sensitive, specific, low-threshold, easily accessible, and cost-effective pathogen detection method. Using SERS for rapid identification of pig pathogens can save detection time, aiming to detect infectious pathogens early and control the spread of diseases. Early detection of pathogens makes it easier to minimize economic losses and achieve early disease eradication (e.g., African swine fever and foot-and-mouth disease), as well as monitor animal epidemics. Given that SERS-related companies are actively promoting its application in the detection of animal diseases and pesticide testing, commercialization is highly probable. This study applies SERS technology to the livestock industry, developing a rapid and highly sensitive pathogen detection method. The sensitivity of SERS in this experiment was approximately 10^2-10^3 CFU/mL, with a detection time of only 30 seconds, although sample pretreatment for a large number of samples (feces, urine, and serum) required 50-95 minutes. For the operation of single or small sample sizes, sample pretreatment can be completed in approximately 10-15 minutes. Therefore, further efforts are needed to shorten the sample pretreatment time for future technology promotion [17].

In comparing SERS technology with current detection methods (such as PCR and ELISA) in terms of relative advantages and cost-effectiveness, firstly, in terms of sample pretreatment, PCR requires more time (extracting DNA or RNA from samples), while SERS technology and ELISA (blood centrifugation, serum dilution, etc.) should be similar. In terms of detection time, SERS technology takes 30 seconds, PCR depends on the program setting (generally taking 1.5-2.5 hours), and ELISA depends on the test setting (generally taking 2.5-4 hours). In terms of cost-effectiveness, when dealing with a small number of samples, the cost of PCR and SERS technology is similar, but ELISA often incurs additional costs due to the design of the kit, resulting in unused reaction wells being discarded, thus increasing the overall cost. Therefore, considering personnel costs, the total cost is: ELISA > PCR or SERS. Additionally, when dealing with a large number of samples, the cost of ELISA decreases, but the time consumption increases, and personnel costs also increase, resulting in a similar cost to SERS technology when converted. SERS technology, on the other hand, has lower personnel costs due to less time spent on subsequent testing, resulting in a lower total cost when combined with personnel costs: PCR > ELISA or SERS [17].

In this experiment, attempts were made to simulate the presence of different target bacteria simultaneously using a known bacterial mouse platform. The results showed that in fecal samples fed with a dual target bacteria, some characteristic wave signals were obscured by other peaks, leading to the phenomenon of unobservable signals. Currently, scholars worldwide have not yet found a solution to this peak obscuration issue. Therefore, in the future, to enhance chip sensitivity, the use of antibody-specificity combined with SERS detection chips could be pursued to address this problem [17].

Since the utilization of SERS requires the establishment of databases for information comparison, to promote the feasibility of SERS application, the short-term goal is to establish a cloud-based system database. With the establishment of the database and optimization of detection requirements, the future vision is for on-site personnel to only require handheld Raman devices for sample pretreatment and detection. Relevant information will be uploaded to the cloud database for comparison, and the matching results will be communicated to on-site personnel via an app. In addition, the efforts will be made to develop artificial intelligence technology simultaneously in the future, aiming for the most user-friendly design to facilitate the promotion of SERS technology.

5. Conclusion

The purpose of this research is to utilize non-invasive real-time imaging systems, coupled with surface plasmon resonance effects and Raman spectroscopy, for application in biomedical molecular detection systems. The aim is to develop novel surface enhancement techniques to monitor the occurrence of animal diseases. Through real-time monitoring, pathogens can be rapidly and accurately detected, thereby initiating the preliminary control of disease spread and reducing economic losses. In the future, this technology will also be applied to specific pathogen-free pigs and the emerging biomedical pig industry. By employing this technology, the goal is to produce experimental pigs with minimal pathogens to meet the demands of the biopharmaceutical industry, thus promoting the development and advancement of the biopharmaceutical industry.

The aim of this study is to utilize a non-invasive real-time spectrum system, coupled with SERS, for biomedical molecular detection applications, with the goal of developing a novel surface enhancement technique to monitor the occurrence of animal diseases. By enabling real-time monitoring, pathogens can be rapidly and accurately detected, thus allowing for the early control of disease spread and reducing economic losses. A standard operating procedure for SERS detection of bacterial pathogens in pigs and zoonotic pathogens, including *Staphylococcus aureus*, *Pseudomonas aeruginosa*, *Salmonella choleraesuis*, *Salmonella typhimurium*, *Actinobacillus pleuropneumoniae*, and *Bordetella bronchiseptica*, has been established. Results have shown that Raman scattering photons exhibit inelastic scattering with a constant Raman shift unrelated to the excitation wavelength of the light source. Using longer wavelengths as the excitation light source provides better wavenumber resolution, while shorter wavelengths result in stronger Raman signals. Raman spectroscopy provides information on substance structure, content, crystallinity, and symmetry of the structure. Proper selection of excitation light sources can avoid fluorescence interference. Laser power should be appropriately controlled to avoid affecting the original characteristics of the sample. Higher grating density leads to higher wavenumber resolution but weaker signals. Shorter wavelengths and higher magnification of the objective lens result in higher spatial resolution. Larger pinholes yield stronger signals but poorer longitudinal resolution. Image mapping can provide spatial distribution information for specific wavenumbers.

SERS detection has been successful in detecting *Staphylococcus aureus*, *Pseudomonas aeruginosa*, *Salmonella choleraesuis*, *Salmonella typhimurium*, *Actinobacillus pleuropneumoniae*, and *Bordetella bronchiseptica*. Further optimization of sample pre-processing methods in detection techniques may reduce noise and increase characteristic peak signals for interpretation. This technology is also applicable to specific pathogen free (SPF) pigs and future

developments in the biomedical pig industry. By producing experimental pigs with minimal pathogen content using this technology, the needs of the biopharmaceutical industry can be met, thereby promoting the development and advancement of the biopharmaceutical industry.

Compliance with ethical standards

Acknowledgments

All authors thank Ministry of Agriculture to provide projects [grant number 106AS-19.3.1-ST-a1, 107AS-15.3.1-ST-a1, and 112AS-2.1.5-AD-U1] for supporting this study.

Disclosure of conflict of interest

The authors declare no conflict of interest.

Statement of ethical approval

The Institutional Animal Care and Use Committee (IACUC) of Agricultural Technology Research Institute inspected all animal experiments and this study comply with the guidelines of protocol IACUC 106112 approved by the IACUC ethics committee.

References

[1] Albrecht MG, Creighton JA. 1977. Anomalously intense Raman spectra of pyridine at a silver electrode. J Am Chem Soc 99: 5215-5217.

[2] Benevides JM, Juuti JT, Tuma R, Bamford DH, Thomas GJJr. 2002. Characterization of subunitspecific interactions in a double-stranded RNA virus: Raman difference spectroscopy of theφ6 procapsid. Biochemistry 41: 11946-11953.

[3] Brakstad OG, Aasbakk K, Maeland JA. 1992. Detection of *Staphylococcus aureus* by polymerase chain reaction amplification of the nuc gene. J Clin Microbiol 30: 1654-1660.

[4] Chen F, Flaherty BR, Cohen CE, Peterson DS, Zhao Y. 2016a. Direct detection of malaria infected red blood cells by surface enhanced Raman spectroscopy. Nanomedicine 12: 1445-1451.

[5] Chen K, Yuen C, Aniweh Y, Preiser P, Liu Q. 2016b. Towards ultrasensitive malaria diagnosis using surface enhanced Raman spectroscopy. Sci Rep 6: 20177.

[6] Cheng IF, Chang HC, Chen TY, Hu C, Yang FL. 2013. Rapid (<5 min) identification of pathogen in human blood by electrokinetic concentration and surface-enhanced Raman spectroscopy. Sci Rep 3: 2365.

[7] Cui S, Zhang S, Yue S. 2018. Raman spectroscopy and imaging for cancer diagnosis. J Healthc Eng 2018: 8619342.

[8] de Planell-Saguer M, M. C. Rodicio MC. 2011. Analytical aspects of microRNA in diagnostics: a review. Anal Chim Acta 699: 134-152.

[9] de Siqueira e Oliveira, Giana FSHE, Silveira LJr. 2012. Discrimination of selected species of pathogenic bacteria using near-infrared Raman spectroscopy and principal components analysis. J Biomed Opt 17: 107004.

[10] Fleischmann M, Hendra PJ, and A. J. McQuillan. 1974. Raman spectra of pyridine adsorbed at a silver electrode. Chem. Phys. Lett 26: 163-166.

[11] Gala UH. 2015. Chauhan. Principles and applications of Raman spectroscopy in pharmaceutical drug discovery and development. Expert Opin Drug Discov 10: 187-206.

[12] Garcia-Rico E, Alvarez-Puebla RA, Guerrini L. 2018. Direct surface-enhanced Raman scattering (SERS) spectroscopy of nucleic acids: from fundamental studies to real-life applications. Chem Soc Rev 47: 4909-4923.

[13] González FJ, Castillo-Martínez C, Martínez-Escanamé M, Ramírez-Elías MG, Gaitan-Gaona FI, Oros-Ovalle C, Moncada B. 2012. Noninvasive estimation of chronological and photoinduced skin damage using Raman spectroscopy and principal component analysis. Skin Res Technol 18: 442-446.

[14] Gorgannezhad L., Umer M, Islam MN, Nguyen NT, Shiddiky MJA. 2018. Circulating tumor DNA and liquid biopsy: opportunities, challenges, and recent advances in detection technologies. Lab Chip 18: 1174-1196.

[15] Hamden KE, Bryan BA, Ford PW, Xie C, Li YQ, Akula SM. 2005. Spectroscopic analysis of Kaposi's sarcoma-associated herpesvirus infected cells by Raman tweezers. J Virol Methods 129: 145-151.

[16] He S, Xie W, Zhang W, Zhang L, Wang Y, Liu X, Liu Y, Du C. 2015. Multivariate qualitative analysis of banned additives in food safety using surface enhanced Raman scattering spectroscopy. Spectrochim Acta A Mol Biomol Spectrosc 137: 1092-1099.

[17] Hung RC, Chen CC, Lin JW, Chuang HL, Chiu CC, Huang PM, Hung YC, Yang CY, Lin CY, Li CL, Hung SW. 2019. Development of rapid detection of animal pathogens by the surface-enhanced Raman scattering system. J Agric For, National Chiayi 16: 61-84.

[18] Jahn IJ, Žukovskaja O, Zheng XS, Weber K, Bocklitz TW, Cialla-May D, Popp J. 2017. Surface-enhanced Raman spectroscopy and microfluidic platforms: challenges, solutions and potential applications. Analyst 142: 1022-1047.

[19] Jeanmaire DL, Van Duyne RP. 1977. Surface Raman spectroelectrochemistry: Part I. Heterocyclic, aromatic, and aliphatic amines adsorbed on the anodized silver electrode. J Electroanal Chem Interfacial Electrochem 84: 1-20.

[20] Jehlička J, Edwards HGM, Oren A. 2014. Raman spectroscopy of microbial pigments. Appl Environ Microbiol 80: 3286-3295.

[21] Klein CS, Piffer IA, Ceroni da Silva S, Schrank A, Fávero MB, Schrank IS. 2003. Detection of *Actinobacillus pleuropneumoniae* by PCR on field strains from healthy and diseased pigs. Curr Microbiol 46: 443-447.

[22] Lambert PJ, Whitman AG, Dyson OF, Akula SM. 2006. Raman spectroscopy: the gateway into tomorrow's virology. Virol J 3: 51.

[23] Lavenir R, Jocktane D, Laurent F, Nazaret S, Cournoyer B. 2007. Improved reliability of *Pseudomonas aeruginosa* PCR detection by the use of the species-specific ecfX gene target. J Microbiol Methods 70: 20-29.

[24] Lehrach H. 2013. DNA sequencing methods in human genetics and disease research. F1000Prime Rep 5: 34.

[25] Lim JY, Nam JS, Yang SE, Shin H, Jang YH, Bae GU, Kang T, Lim KI, Choi Y. 2015. Identification of newly emerging influenza viruses by surface-enhanced Raman spectroscopy. Anal Chem 87: 11652-11659.

[26] Liu TY, Tsai KT, Wang HH, Chen Y, Chen YH, Chao YC, Chang HH, Lin CH, Wang JK, Wang YL. 2011. Functionalized arrays of Raman-enhancing nanoparticles for capture and culture-free analysis of bacteria in human blood. Nat Commun 2: 538.

[27] Liu YC. 2005. Sandwiched structure of Ag/polypyrrole/Au to improve the surfaced-enhanced Raman scattering. Electro Commun 7: 1071-1076.

[28] Long DA. 2002. The Raman effect: A unified treatment of the theory of Raman scattering by molecules. John Wiley & Sons, Inc., Hoboken, New Jersey.

[29] Luo SC, Sivashanmugan K, Liao JD, Yao CK, Peng HC. 2014. Nanofabricated SERS-active substrates for single-molecule to virus detection *in vitro*: A review. Biosens Bioelectron 61: 232-240.

[30] Maurin M. 2012. Real-time PCR as a diagnostic tool for bacterial diseases. Expert Rev Mol Diagn 12: 731-754.

[31] Mayne ST, Cartmel B, Scarmo S, Jahns L, Ermakov IV, Gellermann W. 2013. Resonance Raman spectroscopic evaluation of skin carotenoids as a biomarker of carotenoid status for human studies. Arch Biochem Biophys 539: 163-170.

[32] Mezzetti A. 2015. Light-induced infrared difference spectroscopy in the investigation of light harvesting complexes. Molecules 20: 12229-12249.

[33] Moor K, Ohtani K, Myrzakozha D, Zhanserkenova O, Andriana BB, Sato H. 2014. Noninvasive and label-free determination of virus infected cells by Raman spectroscopy. J Biomed Opt 19: 067003.

[34] Moore DS, Scharff RJ. 2009. Portable Raman explosives detection. Anal Bioanal Chem 393: 1571-1578.

[35] Murray PR, Baron EJ, Pfaller MA, Tenover FC, Yolken RH. 1995. Bordetella. Manual of Clinical Microbiology 46: 566-573.

[36] Negri P, Choi JY, Jones C, Tompkins SM, Tripp RA, Dluhy RA. 2014. Identification of virulence determinants in influenza viruses. Anal Chem 86: 6911-6917.

[37] Neugebauer U, Rösch P, Popp J. 2015. Raman spectroscopy towards clinical application: drug monitoring and pathogen identification. Int J Antimicrob Agents 46 Suppl 1: S35-S39.

[38] Ong YH, Lim M, Liu Q. 2012. Comparison of principal component analysis and biochemical component analysis in Raman spectroscopy for the discrimination of apoptosis and necrosis in K562 leukemia cells. Opt Express 20: 22158-22171.

[39] Paudel A, Raijada D, Rantanen J. 2015. Raman spectroscopy in pharmaceutical product design. Adv Drug Deliv Rev 89: 3-20.

[40] Radu AI, Kuellmer M, Giese B, Huebner U, Weber K, Cialla-May D, Popp J. 2016. Surface-enhanced Raman spectroscopy (SERS) in food analytics: Detection of vitamins B2 and B12 in cereals. J Talanta 160: 289-297.

[41] Renvoisé A, Brossier F, Sougakoff W, Jarlier V, Aubry A. 2013. Broad-range PCR: past, present, or future of bacteriology? Med Mal Infect 43: 322-330.

[42] Rivera SM, Canela-Garayoa R. 2012. Analytical tools for the analysis of carotenoids in diverse materials. J Chromatogr A 1224: 1-10.

[43] Rohr TE, Cotton T, Fan N, Tarcha PJ. 1989. Immunoassay employing surface-enhanced Raman spectroscopy. Anal Biochem 182: 388-398.

[44] Ruokola P, Dadu E, Kazmertsuk A, Häkkänen H, Marjomäki V, Ihalainen JA. 2014. Raman spectroscopic signatures of echovirus 1 uncoating. J Virol 88: 8504-8513.

[45] Saade J, Pacheco MTT, Rodrigues MR, Silveira LJr. 2008. Identification of hepatitis C in human blood serum by near-infrared Raman spectroscopy. Spectroscopy 22: 387-395.

[46] Salman A, Shufan E, Zeiri L, Huleihel M. 2014. Characterization and detection of Vero cells infected with herpes simplex virus type 1 using Raman spectroscopy and advanced statistical methods. Methods 68: 364-370.

[47] Salmon SA, Watts JL, Case CA, Hoffman LJ, Wegener HC, Yancey RJJr. 1995. Comparison of MICs of ceftiofur and other antimicrobial agents against bacterial pathogens of swine from the United States, Canada, and Denmark. J Clin Microbiol 33: 2435-2444.

[48] Singh P, Pandit S, Mokkapati VRSS, Garg A, Ravikumar V, Mijakovic I. 2018. Gold nanoparticles in diagnostics and therapeutics for human cancer. Int J Mol Sci 19: pii: E1979.

[49] Snook RD, Harvey TJ, Correia Faria E, Gardner P. 2009. Raman tweezers and their application to the study of singly trapped eukaryotic cells. Integr Biol (Camb) 1: 43-52.

[50] Stenton SL, Prokisch H. 2018. Advancing genomic approaches to the molecular diagnosis of mitochondrial disease. Essays Biochem 62: 399-408.

[51] Sun Y, Xu L, Zhang F, Song Z, Hu Y, Shen YJiJ, Li B, Lu H, Yang H. 2017. A promising magnetic SERS immunosensor for sensitive detection of avian influenza virus. Biosens Bioelectron 89: 906-912.

[52] Tien N, Chen HC, Gau SL, Lin TH, Lin HS, You BJ, Tsai PC, Chen IR, Tsai MF, Wang IK, Chen CJ, Chang CT. 2016. Diagnosis of bacterial pathogens in the dialysate of peritoneal dialysis patients with peritonitis using surface-enhanced Raman spectroscopy. Clin Chim Acta 461: 69-75.

[53] Thomas GJJr. 1999. Raman spectroscopy of protein and nucleic acid assemblies. Annu Rev Biophys Biomol Struct 28: 1-27.

[54] Urumese A, Jenjeti RN, Sampath S, Jagirdar BR. 2016. Colloidal europium nanoparticles via a solvated metal atom dispersion approach and their surface enhanced Raman scattering studies. J Colloid Interface Sci 476: 177-183.

[55] Wachsmann-Hogiu S, Weeks T, Huser T. 2009. Chemical analysis *in vivo* and *in vitro* by Raman spectroscopy-from single cells to humans. Curr Opin Biotechnol 20: 63-73.

[56] Wang Y, Ruan Q, Lei ZC, Lin SC, Zhu Z, Zhou L, Yang C. 2018. Highly sensitive and automated surface enhanced Raman scattering-based immunoassay for H5N1 detection with digital microfluidics. Anal Chem 90: 5224-5231.

[57] Yi JJ, Park K, Kim WJ, Rhee JK, Son WS. 2018. Spectroscopic methods to analyze drug metabolites. Arch Pharm Res 41: 355-371.